ACADEMIC PRESS

Available online at www.sciencedirect.com
SCIENCE DIRECT®

Journal of Catalysis 219 (2003) 219–230

JOURNAL OF CATALYSIS

www.elsevier.com/locate/jcat

Dynamic phenomena during the photocatalytic oxidation of ethanol and acetone over nanocrystalline TiO_2: simultaneous FTIR analysis of gas and surface species

Juan M. Coronado,*[,1] Sho Kataoka, Isabel Tejedor-Tejedor, and Marc A. Anderson *

Environmental Chemistry & Technology Program, University of Wisconsin at Madison, 660 North Park Street, Madison, WI 53706, USA

Received 21 January 2003; revised 7 April 2003; accepted 16 April 2003

Abstract

Photocatalytic oxidation of acetone and ethanol over nanocrystalline TiO_2 powder was studied under batch conditions using an UV-illuminated DRIFTS chamber as a photoreactor. In this way, we could study the evolution of the reaction by examining changes in the species at the surface of the photocatalyst under UV irradiation. In addition, we were able to simultaneously analyze the gas-phase composition of this reaction by means of a multiple reflection FTIR gas cell. Results obtained indicate that ethanol adsorbs on the TiO_2 surface either molecularly or in the form of ethoxide complexes. Under UV irradiation, these species are progressively removed, and acetate and formate complexes slowly accumulate on the TiO_2 surface. Acetaldehyde builds up in the gas phase during the photocatalytic oxidation of ethanol, although this molecule is scarcely found on the TiO_2 surface. The spectroscopic data provided are consistent with the existence of two parallel reaction pathways for the photocatalytic oxidation of ethanol: one yielding acetaldehyde vapor and the other leading to CO_2 through adsorbed ethoxide species. On the other hand, acetone is adsorbed exclusively in a molecular form on TiO_2. Its photocatalytic oxidation yields acetate and formate complexes, along with adsorbed acetaldehyde and formic acid. These adsorbed molecules can act as intermediates species in the photooxidation of acetone. In addition, participation of specific hydroxyls groups on the TiO_2 surface during this photocatalytic reaction can also be observed using the DRIFTS system.

Keywords: Photocatalysis; Nanoparticles; TiO_2; In situ DRIFTS; Gas-phase FTIR; Surface complexes; Mechanisms; Kinetic model; Acetone; Ethanol

1. Introduction

Photocatalytic oxidation (PCO) of organic pollutants using TiO_2 as a photocatalyst has been extensively studied as a suitable method for the treatment of waste water [1–3]. More recently, it has been recognized that the PCO rates for the gas-phase elimination of certain volatile organic compounds (VOC's) can be higher than those observed for the photocatalytic degradation in aqueous solutions [4,5]. Currently, there is increasing interest in the development of more active catalysts based on nanocrystalline TiO_2 [6,7], especially when used in the form of thin films in order to optimize photon absorption [8,9]. This interest is driven by the incipient commercial exploitation of this technology in the treatment of enclosed atmospheres. In this regard, certain problems can be identified in this process and they must be circumvented if photocatalysis should constitute a widely used method for air purification. First, higher photoactivity is warranted, especially when treating persistent chemicals (i.e., pyridine) [10]. Increases in photooxidation rates would also contribute to limiting the production of partially oxidized compounds, some of which can be very noxious (i.e., traces of $COCl_2$ can be produced during the PCO of TCE) [2–4]. Finally, a higher resistance of photocatalysts to deactivation would improve the overall efficiency of the process during prolonged periods of operation [10].

In this context, a better understanding of the mechanism of these photocatalytic reactions at their molecular level could benefit the design of both materials and reactors, thereby allowing one to tailor photocatalytic systems for spe-

* Corresponding authors.
E-mail addresses: jmcoronado@icp.csic.es (J.M. Coronado), nanopor@facstaff.wisc.edu (M.A. Anderson).
[1] Permanent address: Instituto de Catálisis y Petroleoquímica, CSIC, C/Marie Curie s/n, Cantoblanco, 28049 Madrid, Spain

0021-9517/$ – see front matter
doi:10.1016/S0021-9517(03)00199-4

cific applications. With this aim, a number of studies using ESR [11], FTIR [12–17], and NMR [18,19] spectroscopies or thermally programmed techniques [20,21] have been performed. However, due to the complexity of photocatalytic systems, which include solid and gas (or liquid) phases of variable composition under UV irradiation, most of these studies have been performed under idealized conditions of operation. These conditions may not represent those prevalent in real systems. In general, the experimental constraints of these studies promote the adsorption of the organic molecules, usually favoring the formation of unsaturated sites on the TiO_2 surfaces by dehydration [13–15,17,18]. In addition, reduced pressures of oxygen, spatial velocities approaching zero, and discontinuous illumination are typically employed [11–19]. While such experiments provide valuable information concerning these photoassisted surface reactions, the concentrations of adsorbed reactants and products (organic molecules, oxygen, water, etc.) are most likely different from the actual coverage found in working photocatalytic reactors. Consequently, a correlation between the observed surface reactions and the behavior of a photocatalyst as revealed by the analysis of the gas phase may be difficult to establish, or even misleading.

FTIR spectroscopy has been widely used for the study of heterogeneous catalytic processes because it provides a high sensitivity toward surface complexes and a short response time (i.e., a good quality spectrum can be collected in a few seconds) [12,17]. In addition, this technique allows one to detect most of the molecules in the gas phase (homonuclear diatomic molecules like O_2 are the exception), providing that a long optical-path cell is utilized [22,23]. Consequently, the study of both the TiO_2 surface under UV irradiation and the gas-phase composition can be carried out simultaneously by means of FTIR under conditions close to those prevalent in real systems. In fact, the variation in intensity of CO_2 bands in the gas phase, which are frequently detected superimposed on the spectra of the solid phase, has been occasionally used to determine the extent of the photocatalytic reaction [12–14,17]. Alternatively, by using two separate IR cells for the analysis of each phase, we can obtain spectra which have optimal sensitivity and limited interferences with respect to both the gas phase and the solid/gas interface. In the current article, we present results obtained with a recycling reactor designed for the simultaneous monitoring of the gas and surface composition during these photocatalytic reactions. For this study, ethanol and acetone were used as model compounds and were photodegraded using nanocrystalline TiO_2 powders as photocatalysts. The photocatalytic oxidation of these small organic molecules proceeds with high yield and it has been extensively studied under different conditions [10,13,17–27]. These chemicals can be conveniently used as test molecules to explore the capabilities, as well as the possible limitations, of a photoreactor connected to dual FTIR detectors.

2. Experimental

2.1. Catalyst preparation and characterization

The TiO_2 catalyst was prepared using a sol–gel processing approach [27]. Titanium isopropoxide, $Ti(OPr_i)_4$ (Aldrich, Milwaukee, WI), was added to an aqueous solution of nitric acid at a volumetric mixing ratio of 1 HNO_3:136.4 H_2O:11.4 $Ti(OPr_i)_4$, and immediate precipitation occurred. This suspension was stirred continuously for 3 days until it became a stable clear sol. The acidic sol was dialyzed (Spectra/Por 3 membrane, 3500 MW cutoff, Spectrum, Laguna Hills, CA) to a final pH of 3.5. Subsequently the sol was dried at 60 °C for overnight leading to the production of a xerogel. This xerogel was calcined at 623 K for 3 h with a temperature increasing rate of 3 K per minute. The obtained TiO_2 microporous chips were ground in an agate mortar to a fine powder.

The N_2 isotherm at 77 K of the resulting powders was measured in a Micromeritics ASAP 2010 micropore analyzer (Norcross, GA). From these results, a specific surface area of ca. 160 $m^2\,g^{-1}$, a porosity of 35%, and a mean pore diameter of 4 nm were obtained. The crystal structure of these TiO_2 powders was determined by XRD in a Scintag diffractometer using Cu-K_α radiation. These data indicate that the resulting TiO_2 material is mainly anatase (rutile content is estimated to be ca. 30% according to the relative intensities of the XRD peaks) with an average crystalline size of 10 ± 2 nm.

2.2. Reactor apparatus with dual FTIR detection

Simultaneous FTIR analysis of both the catalyst surface and the gas-phase species was carried out using the reactor assembly schematically shown in Fig. 1. It consisted of two IR cells, a peristaltic pump (MasterFlex Model 7520-10, Cole Palmer, Vernon Hills, IL), and an injecting port (Thermolite Septa, Restek Corp., Bellefonte, PA), which were connected with $\frac{1}{4}$ ft. Teflon tubing. The analysis of the surface of the TiO_2 powder was performed using the diffuse reflectance Fourier transform spectroscopy (DRIFT) mode. The corresponding accessories were the Spectra-Tech (Model 0030-005) system of mirrors for collecting the diffuse IR radiation and a high temperature/vacuum environmental chamber (Model 0030-101, Thermo Spectra-Tech, Shelton, CT) attached to the Teflon line by means of adequate reduction fittings. The stainless-steel dome-shaped top part of the chamber contains two BaF_2 windows, which are transparent in both the IR and the UV ranges (10,000–700 cm^{-1}). Inside the cell, we placed about 30 mg of the catalyst on top of a porous ceramic cylinder, through which gaseous reactants could permeate. The ceramic cylinder is attached to a heater cartridge and a to a K-type thermocouple, both connected to an electronic controller (Thermo Spectra-Tech 0019-22). These devices, in conjunction with

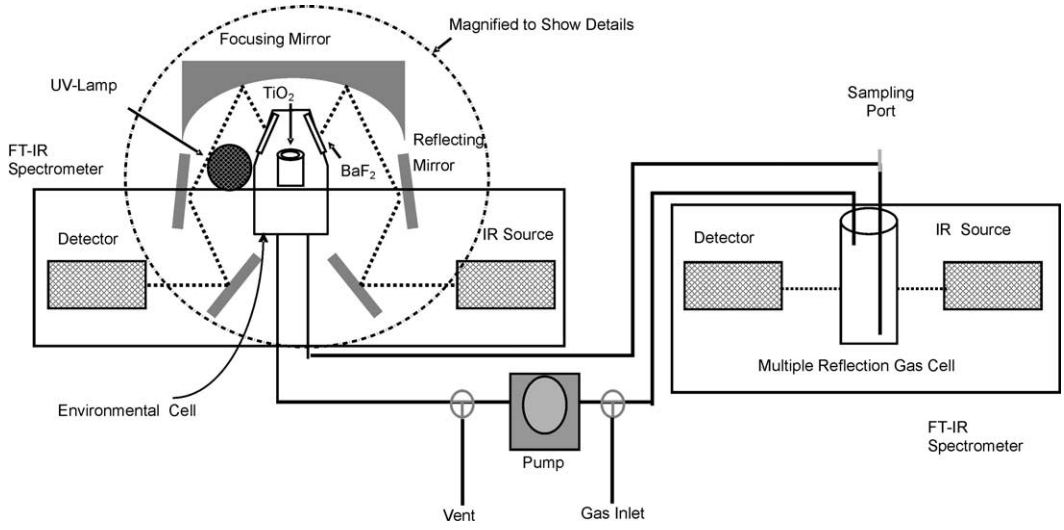

Fig. 1. Schematic diagram of the system used for the in situ simultaneous analysis of the surface and gas species during photocatalytic oxidation of acetone and ethanol. Components are not drawn at scale.

a water-cooling system, provided accurate temperature control (±1 K) for the sample which might otherwise overheat during irradiation. UV illumination of the TiO_2 sample was supplied by a medium pressure Hg vapor lamp (Model 7825-32, 200-W, Ace Glass, Vineland, NJ). The lamp was placed underneath the mirror system in such a way that, despite some shading, the hemispherical mirror could focus part of the radiation on the TiO_2 powder. A light intensity probe (Model IL 1400 with Super-Slim probe in the 250 to 400-nm wavelength range, International Light, Newburyport, MA) was used to test the irradiance on the surface of the sample and was estimated to be ca. 0.12 mW cm^{-2}. Consequently, in this arrangement, the DRIFT environmental chamber can be considered to be a photocatalytic microreactor. However, the efficiency of this system is limited since only the external layer of the catalyst bed is illuminated and consequently low conversions are to be expected. On the other hand, the simultaneous analysis of the gas phase was performed using a 4.8-m permanently aligned FTIR multiple-reflection gas sample cell (Model 4.8-PA, Infrared Analysis Inc., Anaheim, CA). Calibration factors were determined by sampling the gas in the photoreactor loop and obtaining the concentrations with a GC (Hewlett-Packard 5890 Series II, fitted with both TCD and FID detectors) for CO_2 and organic vapors.

In a typical experiment, the reactor loop was flushed at 308 K with a high flow (∼ 150 cm^3 min^{-1}) of dry air (zero air; RH < 0.2%) until the intensity of the bands corresponding to adsorbed water (i.e., bending mode at 1630 cm^{-1}) did not change. Subsequently, the loop was closed, the recycling pump turned on, and a measured amount of the target organic (0.5–1 μL) was spiked into the system. Once the concentration of ethanol (absolute > 99.8%, Aldrich, Milwaukee, WI) or acetone (distilled prior to its use in order to remove dissolved water, Aldrich, Milwaukee, WI) reached a steady value, the lamp was ignited. Simultaneous analysis of the gas and solid surfaces was performed through the dark and illuminated periods at different time intervals. Typical photocatalytic degradation experiments were followed for approximately 4 h.

2.3. Fourier transform infrared spectroscopic analysis

Two different infrared spectrometers were utilized for the analysis of the constituents of gas phase (Magna 750 series II, Nicolet Instruments, Madison, WI) and the surface of TiO_2 (Nexus 670, Nicolet Instruments, Madison, WI). Both instruments were equipped with a globular source and a MCT-A (HgCdTe) detector cooled with liquid N_2. In the case of the gas phase, spectra were recorded in absorbance units after the collection of 50 interferograms with a resolution of 4 cm^{-1}. The single beam spectrum of the cell purged with dry air was used as a background. For the DRIFT analysis of the TiO_2 surface, the resolution was also 4 cm^{-1} but the number of scans was increased to 250. In the case of the solid surface analysis, the background spectrum was collected after a convenient attenuation of the IR beam and placing a mirror on the sample holder. The spectra are displayed in Kubelka–Munk units. The optical path was kept free of ambient CO_2 and water contributions by flowing zero air through the spectrometer.

3. Results

3.1. Adsorption of acetone and ethanol vapors on hydrated TiO_2

After conditioning with a dry air stream, the TiO_2 surface still retains a considerable amount of chemisorbed water, as indicated by the broad band centered at about 3400 cm^{-1} (symmetric and antisymmetric ν(OH) modes) and a sharper one at 1630 cm^{-1} (bending mode) in the DRIFT spectra (not

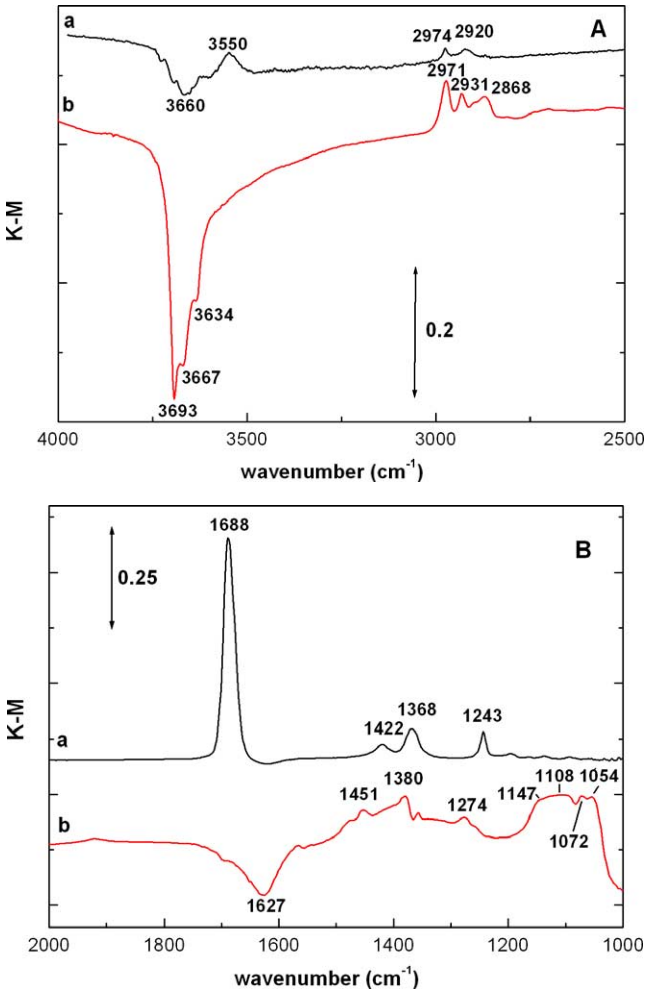

Fig. 2. DRIFT spectra of adsorbed (a) acetone and (b) ethanol on nanocrystalline TiO_2 in the (A) 4000–2500 cm^{-1} and (B) 2000–1000 cm^{-1} range. The spectrum of the solid conditioned in dry air at RT was subtracted from the spectra.

shown). This is in accordance with previous spectroscopic and thermogravimetric studies [16,27,28]. In addition, the bands at 3693, 3667, and 3634 cm^{-1} (appearing as negative peaks in Fig. 2A,b) reveal the presence of several types of isolated OH groups in the hydrated TiO_2 [16,28]. In order to more precisely identify changes in surface composition, the spectrum of the TiO_2 equilibrated in dry air was taken as a reference and subtracted from those obtained after adding the organic vapors. Immediately after introducing organic molecules into the reactor, the intensities of the bands corresponding to the surface complexes rise, meanwhile those of the gas-phase species decrease in a parallel way. However, after an equilibration period of about 40 min, the concentration of all species reaches a steady value and no new products can be detected in the gas phase. Consequently, it can be concluded that neither acetone nor ethanol are oxidized over TiO_2 in the dark.

In the case of acetone adsorption ($\sim$ 14 µmol), the spectrum of TiO_2 obtained after exposure for 50 min to the organic vapors is displayed in Figs. 2A and B,a, and shows positive bands at 3550, 2974, 2920, 1688, 1420, 1368, 1243, 1195, and 1138 cm^{-1}. All these bands, except those at larger frequencies, correspond to molecularly adsorbed acetone, and their assignments are given in Table 1. These values are in accordance with previous reports within a 3 cm^{-1} interval [13] (smaller than the spectral resolution, 4 cm^{-1}). The slight variations in the frequency are very likely related to small changes in the coverage and/or experimental conditions. The peak at 3550 cm^{-1}, along with the negative bands centered at 3660 and 1619 cm^{-1}, account for the modification of the H_2O and OH groups by acetone adsorption. The band at 3550 cm^{-1} can be attributed to those hydroxyls groups interacting with acetone molecules through hydrogen bonding. Therefore, the negative band at 3660 cm^{-1} can be explained rather as a consequence of the transfer of intensity to the lower frequency feature than as due to the depletion of hydroxyls groups. Similar justification has been proposed for the shift of the OH-stretching bands to lower frequencies after adsorption of aromatic molecules on TiO_2 [16,30]. Nevertheless, acetone adsorption may also result in the displacement of a limited amount of adsorbed water. This partial removal of water molecules is suggested by the negative band occurring at 1619 cm^{-1}, which can be related to the low-frequency wing of its bending mode. Furthermore, the interaction between adsorbed acetone and water molecules is revealed by the shift of the band corresponding to the ν(C=O) mode of acetone as function of the hydration state of the TiO_2 surface. This spectral feature appears at 1689 cm^{-1} in hydrated conditions and at 1702 cm^{-1} for the

Table 1
Assignment of the FTIR bands observed upon adsorption of ethanol and acetone vapors on nanocrystalline TiO_2 conditioned in dry air at RT

Adsorbed molecule	Vibration mode	Frequency (cm^{-1})	
		This work	Literature
Acetone[a]	ν(C–H)	2974, 2931	2973, 2931[c]
	ν(C=O)	1688	1702–1689[c]
	$\delta_{as}(CH_3)$	1420	1422[c]
	$\delta_s(CH_3)$	1368	1366[c]
	ν(C–C)	1243, 1195, 1136	1240[c]
Ethanol, Ethoxide[b]	ν(C–H)	2971, 2931, 2868	2971, 2931, 2868[d]
Ethoxide[b]	$\delta(CH_2)$ scissoring	1474	1473[d]
Ethoxide[b]	$\delta_{as}(CH_3)$	1451	1447[d]
Ethoxide[b]	$\delta_a(CH_3)$	1380	1379[d]
Ethoxide	CH_2 wagging	1356	1356[d]
Ethanol[b]	δ(OH)	1274	1264[d]
Ethoxide[b]	ν(C–O) monodent.	1147	1144[d]
Ethoxide[b]	ν(C–O)monodent.	1111	1119[d]
Ethanol[b]	ν(C–C)	1100	1093[d]
Ethoxide[b]	ν(C–C)	1074	1074[d]
Ethoxide[b]	ν(C–O) bridged	1054	1042[d]

[a] Acetone adsorption.
[b] Ethanol adsorption.
[c] Reference [13].
[d] Reference [14].

dehydrated sample [13]. On the other hand, it is worth noting that none of the observed peaks can be attributed to mesityl-oxide, which has been previously observed upon acetone adsorption on dehydrated TiO_2 [13].

The spectrum acquired after adding a small injection of ethanol ($\sim$ 17 µmol) into the system and its subsequent equilibration after 40 min in dry air is shown in Fig. 2,b. Positive bands appears at 2971, 2931, 2868, 1474, 1451, 1380, 1274, 1147, 1111, 1100, 1074, and 1054 cm^{-1}. According to the literature [14], these features can be assigned to the vibration modes of both molecularly adsorbed ethanol (CH_3–CH_2OH) and ethoxide (CH_3–CH_2O^-) species, as outlined in Table 1. The existence of a different set of bands related to the ν(C–O) vibration mode reveals that ethoxide forms two different surface complexes as they bind either to a single (monodentate) or to two (bridged) Ti^{4+} centers [14]. On the other hand, a significant shift to higher frequencies is observed for bands corresponding to molecular ethanol (1274 and 1110 cm^{-1}) with respect to previous values of ethanol adsorption reported for dehydrated TiO_2 [14]. This displacement is very likely related, as proposed in the case of acetone adsorption, to the interaction of the alcohol molecules with water adsorbed on the TiO_2 surface. In any respect, the adsorption of ethanol led to the depletion of isolated OH groups, as indicated by the intense negative band at 3693 cm^{-1} with shoulders at 3667 and 3634 cm^{-1}. In contrast with the case of acetone adsorption, the loss of these features is not accompanied by the generation of a new positive band, suggesting that OH groups are removed rather than perturbed by hydrogen bonding. This fact, along with the detection of ethoxide groups, indicates that upon ethanol admission the following reactions take place:

$$CH_3\text{–}CH_2OH + Ti^{4+}\text{–}OH \rightarrow Ti^{4+}\text{–}O\text{–}CH_2\text{–}CH_3 + H_2O \quad \text{(monodentate)}, \qquad (1)$$

$$CH_3\text{–}CH_2OH + (Ti^{4+})_2\text{–}OH \rightarrow (Ti^{4+})_2\text{–}O\text{–}CH_2\text{–}CH_3 + H_2O \quad \text{(bridged)}. \qquad (2)$$

Similarly, adsorbed water can be partly substituted by alcohol/alkoxide molecules, giving rise to the negative peak at 1627 cm^{-1}. The relatively high intensity of this inverse band suggests a strong competition for adsorption between ethanol and water molecules for reaction sites. This observation is consistent with previous TPD studies that showed a negative correlation between the ethanol concentration on the TiO_2 surface and the relative humidity of the carrier gas [20,21].

3.2. *In situ FTIR study of photocatalytic oxidation of ethanol over TiO_2*

Once the adsorption of ethanol reached equilibrium, as indicated by the steady intensity of the spectra, the UV lamp was ignited. The DRIFT spectra obtained in situ during the photocatalytic oxidation of ethanol vapor over TiO_2 are displayed in Fig. 3 in different ranges. As the spectrum of the

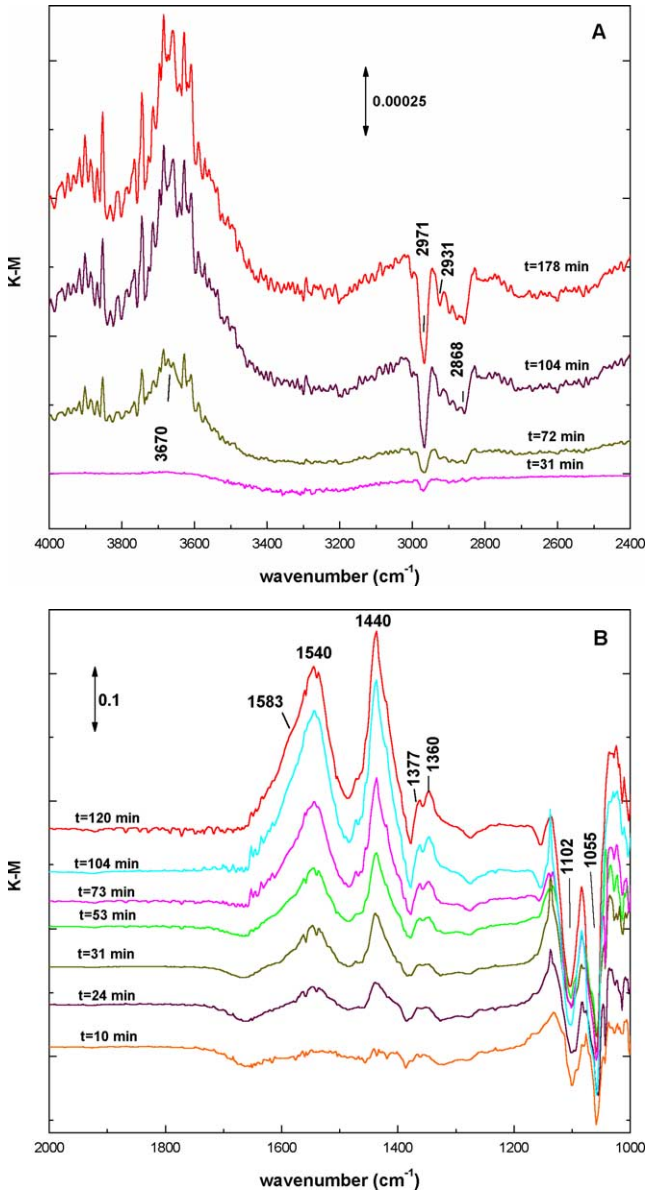

Fig. 3. (A,B) DRIFT spectra obtained in situ during the photocatalytic oxidation of ethanol vapor over TiO_2 powder. The spectrum of the TiO_2 sample equilibrated with ethanol in the dark was subtracted from the spectra.

TiO_2 sample equilibrated in the dark was taken as a background, positive bands represent species generated during the photocatalytic reaction. Meanwhile, negative features of the spectra are related to the depletion of adsorbed species. Thus, the most prominent effect of UV irradiation is the progressive development of bands at 1540 and 1440 cm^{-1}. However, weaker peaks also appear at about 3670 (very broad), 1377, 1360, and 1137 cm^{-1}. In addition, negative bands are observed at 2971, 2931, 2868, 1380, 1274, 1152, 1102 and 1055 cm^{-1}. The extremely sharp peak that is randomly observed at 1138 cm^{-1} is a spurious signal produced by the UV lamp, as confirmed by blank experiments using nonphotoactive KBr powder in air.

According to previous results taken from the literature, bands at 1540 and 1440 cm^{-1} can be assigned to the ν_{as}(COO) and ν_{a}(COO) modes, respectively, of adsorbed acetate complexes [17,29]. However, the marked asymmetry of the high-frequency peak suggests that additional contributions are present. The profile of the spectra obtained under UV irradiation can be fairly well fit with four Gaussian lines (not shown), corresponding to two different surface complexes: bridged bidentate acetate with bands at 1582 and 1417 cm^{-1} and quelate bidentate acetate with bands at 1540 and 1439 cm^{-1} [13,29]. Nevertheless, more detailed studies would be necessary to confirm the presence of these two carboxylate complexes with different geometry. In addition, the peak at 1360 cm^{-1} can be ascribed to the ν_{s}(COO) mode of adsorbed formate species [13,14,29]. These assignments are summarized in Table 2. On the other hand, most of the negative bands can be related to ethoxide complexes (1380, 1152, 1102, and 1055 cm^{-1}), adsorbed ethanol (1274 cm^{-1}), or both (2971, 2931, and 2868 cm^{-1}). In contrast, the broad positive band centered at about 3670 cm^{-1} (Fig. 3A) reveals the progressive development during UV irradiation of surface OH groups. This feature is most likely related to the production of water during the photooxidation, although the decrease of the concentration of molecularly adsorbed ethanol may also modify the profile of the spectra in this region. On the other hand, the negative bands at 1155 and 1102 cm^{-1} (Fig. 3B) indicate that bridged ethoxide species are selectively photooxidized under these conditions. In contrast, previous studies have found that, in the absence of ethanol vapor, the rate of decomposition of the monodentate ethoxide is 1.5 higher than that of the bridged complexes [14]. Finally, it is worth noting that these results suggest that an additional reorganization of the ethoxide species occurs under UV irradiation. Thus, although the intensity of bridged ethoxide (band at 1155 cm^{-1}) complexes progressively decreases a new positive band at about 1137 cm^{-1} first increases and later declines (Fig. 3B).

Table 2
Assignment of the FTIR bands generated during the photocatalytic oxidation of ethanol and acetone vapors over nanocrystalline TiO_2

Surface complexes	Vibration mode	Frequency (cm^{-1})	
		This work	Literature
Formate	ν_{as}(COO) + δ(CH)	2957[a]	2957[c]
	ν_{s}(CH)	2873[a]	2870[c]
	ν_{as}(COO)	1554[a]	1559[c], 1557[d]
	δ(CH)	1381[a]	1385[d]
	ν_{s}(COO)	1360[a]	1358[c], 1371[d]
Acetate	ν_{as}(COO)	1527[a], 1540[b], 1583[b]	1535[e]
	ν_{s}(COO)	1441[a], 1437[b], 1415[b]	1453[e]
Acetaldehyde	ν(C=O)	1715[a]	1718[f]

[a] Acetone photooxidation.
[b] Ethanol photooxidation.
[c] Reference [13].
[d] Reference [14].
[e] Reference [17].
[f] Reference [30].

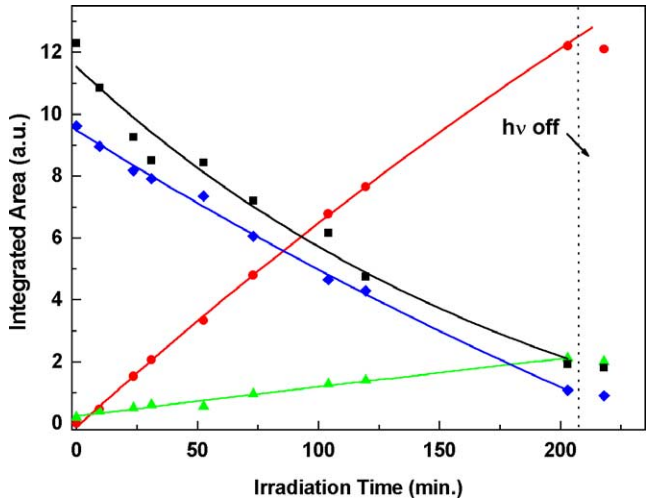

Fig. 4. Variation of the relative intensity of some representative bands of different species adsorbed on TiO_2 during the photocatalytic oxidation of ethanol: (■) ethoxide; bands at 1102 and 1055 cm^{-1}; (◆) ethanol + ethoxide; band at 2970 cm^{-1}; (●) acetate; band at 1540 cm^{-1}; and (▲) formate; band at 1440 cm^{-1}.

The evolution of the integrated area of some of these bands as a function of irradiation time is plotted in Fig. 4. In the absence of systematic adsorption studies, the actual concentration of surface species cannot be determined, since the molar absorption coefficient of the distinct surface species is unknown. Nevertheless, the trend of variation with irradiation time can provide valuable information about the photocatalytic reaction mechanism. The intensity of the bands of photogenerated surface species (acetates and formates) increases with irradiation time, meanwhile ethoxide complexes and adsorbed ethanol molecules are progressively removed. Assuming that the rate of formation/depletion of a generic surface species, A, depends on its surface concentration, and considering that the partial pressure of oxygen remains constant during this process, a pseudo-first-order rate equation can be written,

$$r_A = d\theta_A/dt = k_{app}\theta_A, \quad (3)$$

where r_A is the reaction rate, k_{app} is an apparent kinetic constant, t the time, and θ_A the surface coverage. Since the surface concentration must be proportional to the intensity of the bands of the surface complex A, we can rewrite Eq. (3) as

$$r_A = k_{app} f I_A, \quad (4)$$

where f is a response factor that is related to the molar extinction coefficient, and I_A represents the area of the corresponding IR band. After integration with the adequate initial conditions we have

$$\ln[I_A/I_{A0}] = k_{app}t, \quad (5)$$

where I_{A0} is initial area of the IR band. It is worth noting that the response factor, f, does not appear in the integrated equation and consequently k_{app} can be obtained from the

DRIFTS data, despite the fact that the molar extinction coefficients of the adsorbed species have not been determined [14,17]. Obviously, the validity of the constant, k_{app}, is limited to the particular conditions of the experiment as it depends on several parameters including the photoirradiance, the mass of the catalysts, and the partial pressure of oxygen. The least-square fitting of the experimental results to Eq. (5) is shown in Fig. 4, and it yields a value of 2.6×10^{-4} and 3.5×10^{-4} min^{-1} for the apparent kinetic constant of the formation of acetate (band at 1440 cm^{-1}) and formate (band at 1360 cm^{-1}) complexes, respectively. Similarly, the kinetic constant for the removal of ethoxide complexes is 5.1×10^{-3} min^{-1}, meanwhile the overall constant for the elimination of both molecularly adsorbed ethanol and ethoxide (band at 2971 cm^{-1}) is 2.2×10^{-3} min^{-1}. Therefore, despite the limitations of this simple model, these results suggest that the rate of consuming ethoxide species during UV illumination is significantly larger than the rate of photogenerating adsorbed products.

The simultaneously obtained spectra of gas-phase species are displayed in Fig. 5. The photocatalytic oxidation of ethanol proceeds with evolution of water (not shown), CO_2, and acetaldehyde. Under these conditions, the conversion of ethanol vapor obtained after 220 min is about the 10.5%. The variation during irradiation in the carbon balance, expressed as the difference between the ethanol consumption and the CO_2 and acetaldehyde production, is also represented in Fig. 5. These results indicate that a certain accumulation of organic compounds on the surface of TiO_2 occurs during the initial period of irradiation, but subsequently, the amount of surface carbon remains basically constant. Thus, gas-phase species account for about the 81% of the ethanol eliminated just before turning off the lamp. The coverage of ethanol of the TiO_2 surface, θ_{Eth}, can be calculated according to the

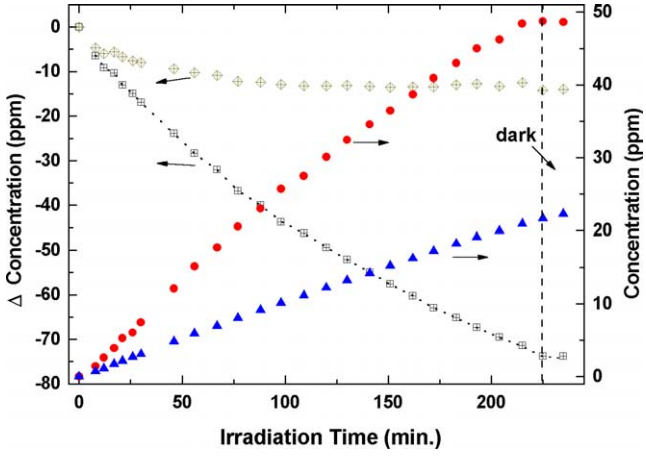

Fig. 5. Variation of the gas-phase concentration of different molecules during the photocatalytic oxidation of ethanol on TiO_2: (⊞) ethanol; (●) acetaldehyde; and (▲) CO_2. The difference between the ethanol transformed and the acetaldehyde and CO_2 produced is represented as ⊕. The dotted line corresponds to the Langmuir–Hinselwood–Hougen–Watson plot of the ethanol vapor data.

Langmuir adsorption isotherm as

$$\theta_{Eth} = K P_{Eth}/(1 + K P_{Eth}), \quad (6)$$

where P_{Eth} is the ethanol partial pressure. Since the ethanol concentration used is small, Eq. (6) can be rewritten as

$$\theta_{Eth} \approx K P_{Eth} = f' I_{Eth}, \quad (7)$$

where I_{Eth} is the intensity of a specific band of the gas spectra, and f' a response factor. After substitution of this formula in Eq. (3) and subsequent integration, an expression equivalent to Eq. (5) is obtained,

$$\ln[I_{Eth}/I_{Eth0}] = k_{app} t, \quad (8)$$

where I_{Eth0} is the initial intensity of the corresponding ethanol band. The fit of the ethanol vapor data to this formula yields a value of $k_{app} = 2.9 \times 10^{-3}$ min^{-1}, which is close to that calculated for the removal of adsorbed ethanol ($k_{app} = 2.2 \times 10^{-3}$ min^{-1}). The calculation of an approximate kinetic constant is a means of correlating the results from gas-phase analysis to those obtained by analyzing changes in surface species. However, if the full expression of the dependence of coverage on the ethanol vapor pressure (i.e., Eq. (6)) is used the Langmuir–Hinselwood–Hougen–Watson equation (LHHW) is obtained. As shown in Fig. 5, the LHHW model can adequately describe the experimental data, in accordance with previous reports [1,2,8,9,22,25]. Finally, it is also of note that no apparent deactivation has been observed in the time span of the present study, despite the buildup of adsorbed species on the TiO_2.

3.3. *In situ FTIR study of photocatalytic oxidation of acetone over TiO_2*

Similarly to the ethanol case, the photocatalytic oxidation of acetone started after first attaining adsorption equilibrium. The DRIFT spectra of TiO_2 recorded subsequently under UV irradiation are displayed in Fig. 6. As in the case of ethanol, the spectrum of TiO_2 equilibrated in the dark with acetone vapor was taken as a reference and subtracted from those recorded under illumination. These results show that, under UV irradiation, the intensity of the acetone bands (negative peaks at 1688 and 1054 cm^{-1}) progressively decrease, and simultaneously new strong peaks arise at 2956, 2870, 1715, 1556, 1440, 1379, and 1358 cm^{-1}. Most of these positive bands, whose proposed assignments are summarized in Table 2, can be related to formate ($HCOO^-$) and bidentate acetate (CH_3–COO^-) surface complexes [14,17, 29]. However, the symmetry of the adsorbed formate cannot be definitely established. This is due to the fact that, in the present case, the difference between the frequency of the asymmetric and symmetric ν(COO) modes, which is the parameter that allows one to determine the geometry of carboxylates, is close to the borderline value of 200 cm^{-1} [29]. Thus, the formation of either bridged [14] or bidentate [13] formate complexes on the surface on TiO_2 during photocatalytic oxidation has been proposed previously. On the other

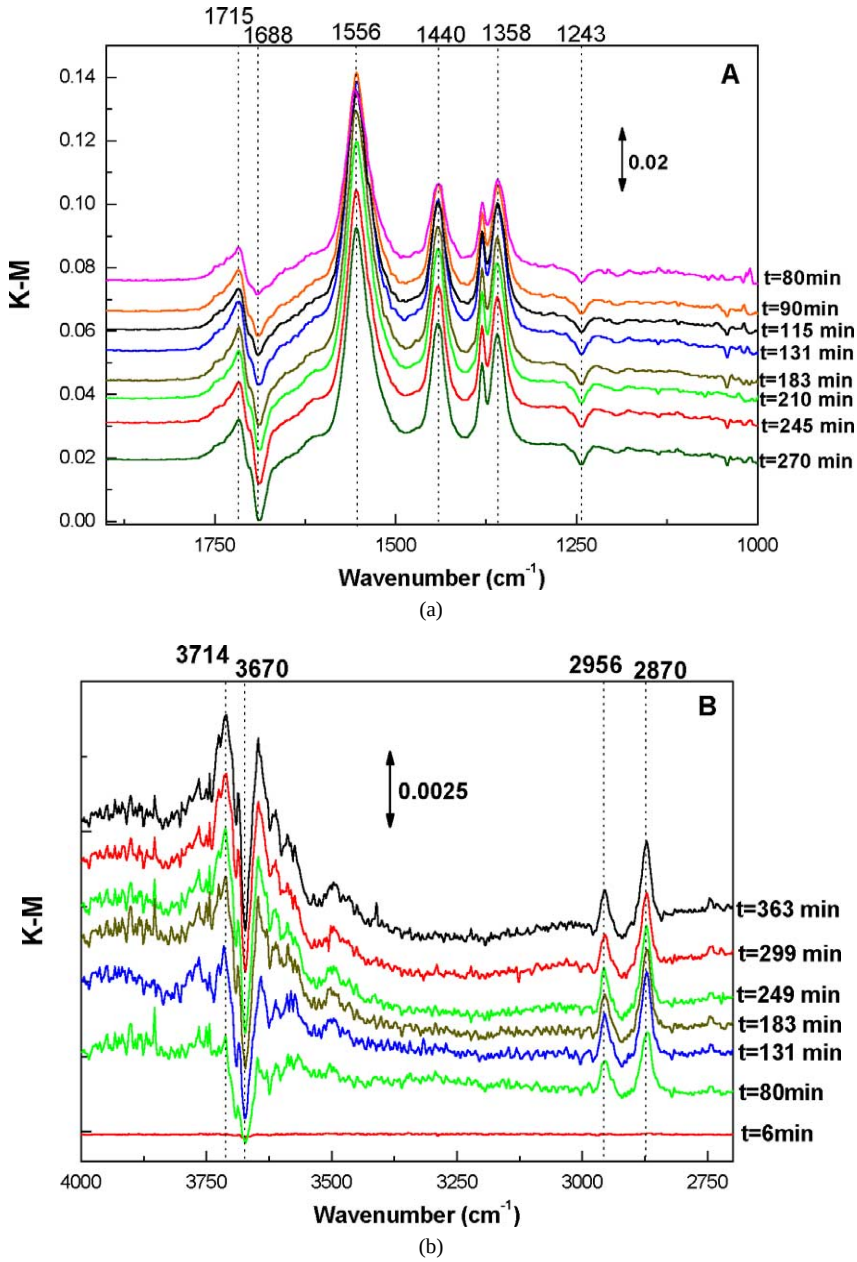

Fig. 6. (A,B) DRIFT spectra obtained in situ during the photocatalytic oxidation of acetone vapor over TiO_2 powder. The spectrum of the TiO_2 sample equilibrated with acetone in the dark was subtracted from the spectra.

hand, El-Maazawi et al. have ascribed the peak at 1440 cm^{-1} to free carbonates [13], but the current results suggests that it corresponds to the ν_s(COO) mode of surface acetate in agreement with other studies [17] and consistently with the results given above for ethanol. Moreover, the subtraction of successive spectra of Fig. 6 reveals the existence of an additional band at $\sim$ 1530 cm^{-1}, whose intensity increment parallels that of the band at 1441 cm^{-1}. Consequently, it can be assumed that the band at 1554 cm^{-1} consists of two contributions corresponding to the ν_{as}(COO) mode of both formate and acetate complexes [14,17]. The position of these overlapping peaks was estimated by deconvoluting the spectra using Gaussian lines, and values obtained are given in Table 2. Finally, the peak at 1715 cm^{-1} can be assigned to the ν(C=O) vibration mode of adsorbed aldehyde. Both formaldehyde and acetaldehyde are plausible intermediates of acetone photocatalytic oxidation, and they could account for the band at 2870 cm^{-1} which is characteristic of the ν(CH) vibration of aldehyde molecules. Nevertheless, the reported frequency for acetaldehyde on TiO_2, 1718 cm^{-1}, is closer to the value obtained in this study [31,32]. Although the interference with formate species prevents one from observing the $\delta(CH_3)$ vibration mode at 1355 cm^{-1} [31], we believe that adsorbed acetaldehyde is very likely formed during photocatalytic oxidation of acetone. On the other hand, the shoulder at ca. 1745 cm^{-1} could correspond to formic

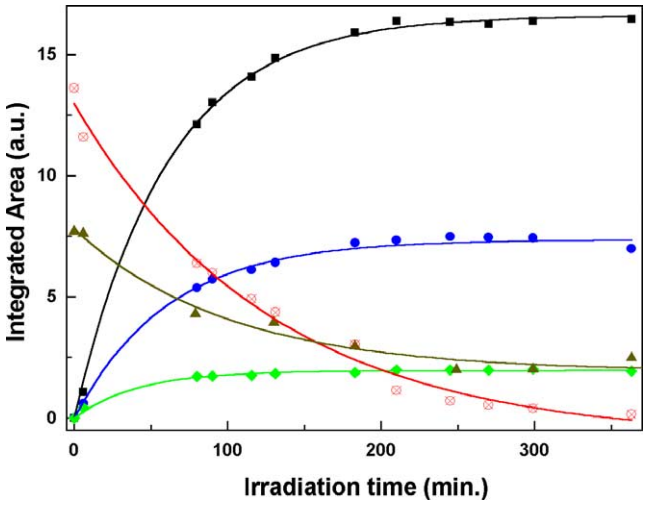

Fig. 7. Variation of the relative intensity of some representative bands of different species adsorbed on TiO_2 during the photocatalytic oxidation of acetone: (■) acetate; (●) formate; (◆) acetaldehyde; (⊗) acetone; and (▲) hydroxyls.

acid, whose dimeric form displays a band at 1740 cm^{-1} [17]. However, the possible formation of acetic acid cannot be ascertained, because the corresponding ν(CO) band overlaps with that of the acetone [17]. Finally, the negative band at 3670 cm^{-1} indicates that some specific OH groups are depleted with increasing irradiation time. In contrast, other sharp bands associated with isolated hydroxyl groups tended to increase in intensity during irradiation. This is likely due to the formation of water as a product of the photocatalytic oxidation of acetone.

The variation with irradiation time of the integrated area of selected bands, which are representative of adsorbed species, is displayed in Fig. 7. Changes in the surface concentration of both carboxylates (monitored by the intensity of the bands at 1550 and 1361 cm^{-1}, respectively), along with acetaldehyde (band at 2850 cm^{-1}), show a similar tendency. The rate of formation of these adsorbed complexes appreciably declines after prolonged irradiation. This behavior indicates that surface has reached a steady state, which may be determined either by the saturation of the adsorption sites and/or by the dynamic equilibrium between the production and the elimination of intermediates. In contrast, the concentration of adsorbed acetone continuously decreases, and considering a first-order kinetic (Eq. (5)), the rate for its removal can be modeled with $k_{app} = 0.021$ min^{-1}. Similarly, the kinetic constant for the elimination of hydroxyls (band at 3670 cm^{-1}) is found to be considerably lower, $k_{app} = 0.010$ min^{-1}. On the other hand, the simultaneous variation in the acetone vapor concentration shows a progressive decrease, in parallel to the increasing CO_2 production. No other product, except water vapor, is detected in the gas phase during the photocatalytic reaction. A kinetic constant of $k_{app} = 0.019$ min^{-1} is obtained by applying the first-order kinetic model to the vapor-phase data. This result is consistent with the value obtained for the removal of adsorbed acetone. Under these experimental conditions, the final conversion of acetone vapor is about the 16%, and CO_2 in the gas phase accounts for the 60% of the acetone removal. These results are in accordance with the significant buildup of partially oxidized products, as detected by DRIFT.

4. Discussion

In addition to acetaldehyde, several studies have identified acetic acid, formaldehyde, and formic acid as intermediates in the photocatalytic oxidation of ethanol [20,21, 32,33]. Although the formation of acetaldehyde is generally considered the first step of the photocatalytic oxidation, there is no general agreement about the reaction pathways that lead to the other by-products. Thus, Nimlos et al. [33] proposed a sequential mechanism in which acetic acid is generated from acetaldehyde and successively transformed into formaldehyde, formic acid, and finally CO_2. Other authors have suggested more complex reaction schemes, where the formation of carboxylic acids and eventually CO_2 occurs through parallel reactions involving both formaldehyde and acetaldehyde [20,32]. Muggli et al. [20,21] have concluded from TPD and isotopic exchange studies that weakly adsorbed ethanol is preferentially photooxidized to acetaldehyde; meanwhile, strongly adsorbed ethanol yields CO_2. These results are basically in agreement with the FTIR investigation of Lin and co-workers [14,17], which have shown that molecularly adsorbed ethanol are transformed upon UV irradiation into acetaldehyde. In contrast, more strongly adsorbed ethoxide complexes are photooxidized to adsorbed acetate and formate [14,17]. In the present study, carbon balance data (see Fig. 5) indicate that by-products (most likely acetate and formate complexes) of the photocatalytic oxidation of ethanol initially accumulate on the surface of the catalyst. However, after prolonged irradiation, the carbon inventory of the TiO_2 surface does not significantly change although the amount of adsorbed carboxylates keeps rising. This observation is consistent with the photocatalytic transformation of ethoxide complexes into carboxylates [14,17], as this surface reaction occurs without increasing the amount of adsorbed carbon. Nevertheless, the apparent kinetic constants for the formation of both surface acetates and formates are an order of magnitude lower than that for removing ethoxide species. This fact suggests that ethoxide complexes experience additional transformations that very likely lead to the formation of CO_2. Therefore, the accumulation of acetates and formates on the surface of TiO_2 could indicate that their transformation into CO_2 occurs at slightly slower rate than their production. On the other hand, it may be argued that, due to the larger penetration depth of the infrared radiation as compared to UV light, accumulation of carboxylates occurs in the dark (non-UV-illuminated) areas of the TiO_2 particles. Similar arguments have been proposed in order to explain the differences in the carbon balance observed

between monoliths and thin films of TiO_2 for the photocatalytic oxidation of ethanol [32]. The process of accumulating organic species in dark areas of the surface could account, at least partially, for the initial decrease of the amount of carbon in the gas phase upon UV irradiation. Nevertheless, the DRIFT results, which show extensive photoinduced transformations of surface complexes, are in agreement with the gas-phase analysis of the photocatalytic reaction, and suggest that the possible contribution of the dark areas is very likely not significant under these conditions.

As other studies have reported [20,21,32,33], the rate of formation of acetaldehyde vapor from the photocatalytic oxidation of ethanol is considerably larger than that of the CO_2 production. Surprisingly, despite the progressive increase in its concentration in the gas phase, the amount of acetaldehyde present on the surface of TiO_2 under the conditions of the present study is very low. In fact, only a weak band at 1715 cm^{-1} can be observed in some of the spectra. These results contrast with the significant concentration of adsorbed acetaldehyde detected during the photocatalytic oxidation of acetone. A possible explanation for such observations is that acetaldehyde adsorption is prevented by ethanol, as has been experimentally found previously [33]. Competition of acetaldehyde molecules for the adsorption sites with strongly bound ethoxide complexes could justify these results. On the other hand, since acetaldehyde is eventually mineralized [32,33], an additional pathway for the photocatalytic oxidation of acetaldehyde must be considered. According to these data, the overall mechanism proposed for the photocatalytic oxidation of ethanol is outlined in the Scheme 1.

Deactivation of catalysts is frequently related to the buildup of unreactive by-products on the active centers of the surface. In the case of the photocatalytic oxidation of ethanol over TiO_2, it has been suggested that the accumulation of adsorbed acetaldehyde and/or related compounds could account for decline in reaction rates [20,21]. However, as noted above, the concentration of acetaldehyde on the surface of TiO_2 is very low under the experimental conditions used in the current study. On the contrary, the concentration of adsorbed acetate and formate complexes continuously increases during the photocatalytic oxidation of ethanol. Effectively, these species are strongly adsorbed on the TiO_2 surface as they are hardly removed by thermal activation [14,17]. Although these complexes are less reactive than ethoxide species, they can be photooxidized [14,17]. Consequently, deactivation is not observed under the conditions of the present study. However, it is possible that if the concentration of the organic target is high, the concentration of adsorbed acetates could limit the access of the reactive molecules to the adsorption sites. Under these circumstances, a decrease of the reaction rate could be expected.

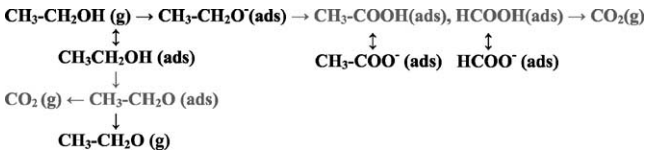

Scheme 1. "↔" represents reversible reactions. Photocatalytic processes are drawn in gray.

Most of the studies concerning the photocatalytic oxidation of acetone have failed to detect any intermediate. El-Maazawi et al. [13] ascribed the species detected by FTIR on the TiO_2 surface during the photooxidation to formate, carbonates, and adsorbed CO_2 and H_2O. In the present study, we also have obtained evidence for the generation of formic acid and acetaldehyde, along with acetate and formate complexes. Although the strong band of ν(CO) of acetone masks the distinctive feature of acetic acid at 1680 cm^{-1} [14], acetic acid may be present as well. In fact, the decrease of the acetone peaks at 1688 cm^{-1} is significantly lower than other bands of this molecule, suggesting the presence of additional contributions in this spectral range. In any case, neither acetaldehyde nor formic acid are detected in the gas phase. This behavior indicates that their desorption rate is considerably lower than the rate for their photocatalytic oxidation. These observations suggest that the acetone molecules break after the attack of the photogenerated charge carriers to yield a two-carbon molecule and a single carbon one. The fact that formic acid and acetaldehyde accumulates on the surface until reaching a steady-state concentration indicates that the limiting step of the photocatalytic oxidation of acetone is the mineralization of such compounds. On the other hand, after an initial rapid increase the concentration of acetate and formate complexes on the TiO_2 surface also achieves a constant value. Since the photocatalytic oxidation rate of theses species is slower than that of their corresponding carboxylic acids [14,17], it can be assumed that the acid–base reactions participate in their transformation. In this way, surface formate and acetate complexes can be in equilibrium with their corresponding acids if some protons are available in the surface. In summary, the overall mechanism that can be envisaged from theses spectroscopic data is outlined in the Scheme 2.

In the case of ethanol, the strong interaction by hydrogen bonding of the alcohol group of the organic molecule with adsorbed water and hydroxyl groups of the TiO_2 surface hinders the analysis of their evolution during the photocatalytic oxidation. Nevertheless, the variation of the DRIFT spectra of Fig. 3A during photocatalytic oxidation of ethanol points to the generation of hydroxyls groups as a consequence of the formation of water. Similarly, in the case of acetone, changes in the ν(OH) range of the spectra provide information concerning the role of adsorbed water in the photocatalytic oxidation of organic pollutants. Thus, although the intensity in the 3800–3600 cm^{-1} range progressively

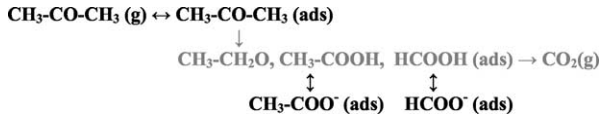

Scheme 2. "↔" represents reversible reactions. Photocatalytic processes are drawn in gray.

increases during UV irradiation; remarkably, the band at 3670 cm^{-1} decreases in a parallel way to the concentration of adsorbed acetone. The $OH^{\cdot}$ radicals, which are formed by trapping of a photogenerated hole by a hydroxyl group of the TiO_2, are generally considered the active species for the photocatalytic oxidation [2,3,11,13,16]. Consequently, the selective removal of the OH^- groups associated with the band at 3670 cm^{-1} could represent their consumption following hole trapping by reaction with acetone molecules. Nevertheless, the nonphotoactivated neutralization reaction of acetic and formic acids with the TiO_2 surface to yield formates and acetates complexes should also contribute to the depletion of hydroxyls groups. The absence of such selective removal of hydroxyl in the case of photooxidizing ethanol may be related to the previous formation of ethoxide complexes. This implies the substitution of several OH groups by CH_3CH_2O– species (reactions (1) and (2)). Although the results shown in Fig. 7 indicate that once the concentration of surface carboxylates reaches a steady state the amount of OH^- still decreases, further studies will be necessary to ascertain the contribution of each process. In any case, the differential removal of a particular type of hydroxyl indicates the specificity of the process involved. Furthermore, as the surface coverage of each OH type depends on the crystallographic plane of the TiO_2 exposed [34], this observation may indicate that the photocatalytic oxidation of acetone may show structural sensitivity. Nevertheless, additional investigations are required in order to confirm these assumptions and to clarify the role of adsorbed water and OH groups on the photoactivity of organic species on the surface of semiconductors.

5. Conclusions

The present results show that the use of a reactor with dual FTIR detection for the simultaneous analysis of gas and surface species can provide a very detailed knowledge of the mechanism of photocatalytic reactions, as it allows one to relate surface processes with changes in gas composition. Nevertheless, quantification and modeling of the data so obtained are significantly limited by the fact that the molar absorption coefficients of surface complexes are generally unknown, and consequently only relative variations in the concentration of these adsorbed species can be attained.

In the present work, the capabilities of such a dual reaction setup were tested for the study of the photocatalytic oxidation of ethanol and acetone vapors. The results presented show that variations in the concentration of the surface complexes formed upon acetone and ethanol adsorption reflect those occurring in the gas phase during UV irradiation. In addition, some species accumulates on the TiO_2 surface, as indicated by the carbon balance in the gas phase and the increment in adsorbed molecules on the TiO_2 surface. However, no apparent deactivation has been observed under the experimental conditions used in this study. Therefore, the identified surfaces complexes do not play a significant role in the poisoning of the active sites, at least in such concentrations. Furthermore, the detected adsorbed species seem to participate actively in the photocatalytic reaction. Thus, acetates and formates are apparently intermediates in the production of CO_2 during the photocatalytic oxidation of ethanol. In the case of acetone, acetaldehyde and formic acid are also observed in the TiO_2 surface. In these reactions, a significant participation of adsorbed OH/H_2O species is envisaged. On the other hand, the main differences between the photocatalytic oxidation of acetone and ethanol are derived from the fact that alcohol molecules react with the TiO_2 surface to yield ethoxide complexes meanwhile acetone is adsorbed molecularly.

Acknowledgments

J.M.C. thanks the Comunidad Autónoma de Madrid (C.A.M.) for the award of a postdoctoral grant. The stay of J.M.C. at the University of Wisconsin was funded by the Estancias Breves program of the C.A.M.

References

[1] A. Mills, R.H. Davies, D. Worsley, Chem. Soc. Rev. (1993) 417.
[2] M.R. Hoffman, S.T. Martin, W. Choi, D.W. Bahnemann, Chem. Rev. 95 (1995) 69.
[3] A. Linsebigler, G. Lu, J.T. Yates, Chem. Rev. 95 (1995) 735.
[4] J. Peral, D. Ollis, J. Catal. 136 (1992) 554.
[5] N.N. Lichtin, M. Avudaithai, Environ. Sci. Technol. 30 (1996) 2014.
[6] H. Kominami, J. Kato, Y. Takada, Y. Doushi, B. Ohtani, S. Nishimoto, M. Inoue, T. Inui, Y. Kera, Catal. Lett. 46 (1997) 235.
[7] A.J. Maira, K.L. Yeung, J. Soria, J.M. Coronado, C. Belver, C.Y. Lee, V. Augugliario, Appl. Catal. B 29 (2001) 327.
[8] A. Sirisuk, C.G. Hill, M.A. Anderson, Catal. Today 54 (1999) 159.
[9] M.E. Zorn, D.T. Tompkins, W.A. Zeltner, M.A. Anderson, Environ. Sci. Technol. 4 (2000) 5206.
[10] R.M. Alberici, W.F. Jardim, Appl. Catal. B 14 (1997) 55.
[11] Y. Nosaka, K. Koenuma, K. Ushida, A. Kira, Langmuir 12 (1996) 736.
[12] J. Zhuang, C.N. Rusu, J.T. Yates Jr., J. Phys. Chem. B 103 (1999) 6957.
[13] M. El-Maazawi, A.N. Finken, A.B. Nair, V.H. Grassian, J. Catal. 191 (2000) 138.
[14] W.C. Wu, C.C. Chuang, J.L. Lin, J. Phys. Chem. B 104 (2000) 8719.
[15] D.V. Kozlov, E.A. Paukshtis, E.N. Savinov, Appl. Catal. B 24 (2000) L7.
[16] A.J. Maira, J.M. Coronado, V. Augugliario, K.L. Yeung, J.C. Conesa, J. Soria, J. Catal. 202 (2001) 413.
[17] L.F. Liao, W.C. Wu, C.Y. Chen, J.L. Lin, J. Phys. Chem. B 105 (2001) 7678.
[18] S. Pilkenton, S.J. Hwang, D. Raftery, J. Phys. Chem. B 103 (1999) 11152.
[19] W. Xu, D. Raftery, J. Catal. 204 (2001) 110.
[20] D.S. Muggli, K.H. Lowery, J.L. Falconer, J. Catal. 180 (1998) 111.
[21] D.S. Muggli, J.T. McCue, J.L. Falconer, J. Catal. 175 (1998) 213.
[22] J.M. Coronado, M.E. Zorn, I. Tejedor-Tejedor, M.A. Anderson, Appl. Catal. B, in press.
[23] A. Dombi, A.Z. Fekete, I. Kiricsi, Appl. Catal. A 193 (2000) L5.

[24] J.C. Kennedy III, A.K. Datye, J. Catal. 179 (1998) 375.
[25] A.V. Vorontsov, I.V. Stoyanova, D.V. Kozlov, V.I. Simagina, E.N. Savinov, J. Catal. 186 (1999) 318.
[26] E.M. Zorn, D.T. Tompkins, W.A. Zeltner, M.A. Anderson, Appl. Catal. B 23 (1999) 1.
[27] F.M. Vichi, M.I. Tejedor-Tejedor, M.A. Anderson, Chem. Mater. 12 (2000) 1762.
[28] C. Morterra, J. Chem Soc. Faraday Trans. 84 (1988) 1617.
[29] N. Nagao, Y. Suda, Langmuir 5 (1989) 42.
[30] J.E. Rekoske, M.A. Barteau, Langmuir 15 (1999) 2061.
[31] G.Y. Popova, T.V. Andrushkevich, Y.A. Chesalov, E.S. Stoyanov, Kinet. Catal. 41 (2000) 805.
[32] M.L. Sauer, D.F. Ollis, J. Catal. 158 (1996) 570.
[33] M.R. Nimlos, E.J. Wolfrum, M.L. Brewer, J.A. Fennell, G. Bintner, Environ. Sci. Technol. 30 (1996) 3102.
[34] M.A. Henderson, Langmuir 12 (1996) 5093.